Journal of Crystal Growth 310 (2008) 4927–4931

Contents lists available at ScienceDirect

Journal of Crystal Growth

journal homepage: www.elsevier.com/locate/jcrysgro

AlGaN/AlN multiple quantum wells grown by MOVPE on AlN templates using nitrogen as a carrier gas

S. Gautier [a,*], T. Aggerstam [b], A. Pinos [b], S. Marcinkevičius [b], K. Liu [c], M. Shur [c], S.M. O'Malley [d], A.A. Sirenko [d], Z. Djebbour [e], A. Migan-Dubois [e], T. Moudakir [f], A. Ougazzaden [f]

[a] Laboratoire Matériaux Optiques, Photonique et Système (LMOPS), UMR CNRS 7132, University of Metz and Supelec, 2 rue Edouard Belin, F-57070 Metz, France
[b] Department of Microelectronics and Applied Physics, Royal Institute of Technology, Electrum 229, SE-164 40 Kista, Sweden
[c] Department of ECSE and CIE, Rensselaer Polytechnic Institute, Troy, NY 12180, USA
[d] Department of Physics, New Jersey Institute of Technology, Newark, NJ 07102, USA
[e] Laboratoire de Génie Electrique de Paris, UMR 8507 CNRS, SUPELEC, University Paris-Sud 11, UPMC, UVSQ-PRES UniverSud, 11 rue Joliot-Curie, Plateau de Moulon, F-91192 Gif-sur-Yvette Cedex, France
[f] Georgia Institute of Technology/GTL, UMI 2958 GT-CNRS, 2-3 rue Marconi, F-57070 Metz, France

ARTICLE INFO

Available online 26 August 2008

Keywords:
A3. Metalorganic vapour phase epitaxy
B1. AlGaN
B1. Nitrides
B2. Semiconducting gallium compounds

ABSTRACT

$Al_xGa_{1-x}N$/AlN multiple quantum wells (MQWs) structures were grown by metalorganic vapour phase epitaxy (MOVPE) on pseudo AlN substrates using nitrogen as a carrier gas. Results of X-ray diffraction (XRD) and reciprocal space mapping (RSM) indicated no sign of strain relaxation in the quantum wells with respect to the AlN substrate. The MQW parameters such as thicknesses, growth rates and material compositions were extracted from XRD measurements and demonstrated an agreement with our growth conditions. No indication of parasitic reactions between ammonia and trimethyl-aluminium (TMAl) was detected in our growth process. Optical measurements revealed well-defined photoluminescence peaks at 288 and 280 nm, which are in a good agreement with the transmission experimental data. The piezoelectric field value in the studied structures was estimated to be 900 kV/cm.

1. Introduction

AlGaN/AlN heterostructures are promising for UV to deep UV laser diodes and photo detectors. Due to the large tensile strain between AlN and GaN, Al-rich AlGaN/GaN superlattices (SLs) grown on GaN templates suffer from cracks or high dislocation density after relaxation [1] leading to lower device output optical power and shorter carrier lifetimes [2]. Further, absorption in the underlying GaN reduces the external quantum efficiency of UV light emitters. A large number of publications have reported on the growth and applications of thick crack-free AlGaN layers on sapphire using AlGaN/AlN buffer structures, but only a few publications have addressed the growth of AlGaN/AlN multiple quantum wells (MQWs) on AlN template substrates [3–5] or on bulk AlN [6]. Such UV-transparent AlN template substrates offer a possibility to grow Al-rich structures with stress-free barriers and, hence, with a reduced global structure strain. In addition, AlGaN/AlN MQWs are favourable for abrupt interfaces compared to conventional AlGaN/GaN structures since the Al compositions in the wells and barriers are close. On the other hand, a high concentration of Al requires a high flow of trimethyl-aluminium (TMAl), which with the presence of ammonia (NH_3) causes parasitic reactions and generates particles [7]. Different growth conditions have been used to address this issue. For instance, it has been shown that a reduced pressure of about 100 mbar, a short distance between gas in-lets and susceptors and a small dead volume are prerequisites [8]. Furthermore, using nitrogen as a carrier gas one can improve the structural quality of quantum well (QW) structures [9]. In this paper, AlGaN/AlN MQWs have been grown at low pressure and with 100% nitrogen as a carrier gas.

2. Experiments

The growth was carried out in a T-shape reactor [10] using TMAl, trimethyl-gallium (TMGa) and NH_3 as precursors for aluminium, gallium and nitrogen, respectively. Hundred percent nitrogen was used as a carrier gas. The growth pressure and the temperature were constant at 135 mbar (100 Torr) and 1000 °C, respectively. Four MQWs structures were grown on 630-nm-thick AlN templates on sapphire. The MQWs consisted of five periods of AlGaN/AlN grown without any interruption between the wells and barriers (see Fig. 1(a)).

* Corresponding author.
E-mail address: simon.gautier@metz.supelec.fr (S. Gautier).

0022-0248/$ - see front matter © 2008 Elsevier B.V. All rights reserved.
doi:10.1016/j.jcrysgro.2008.08.040

If the parasitic reaction between TMAl and NH_3 can be mainly suppressed by using nitrogen as a carrier gas, the incorporation of III elements remained to be sensitive to the flow of NH_3 in the growth chamber. In order to have a good control of the composition in the wells, we have kept a constant V/III ratio of 875 in the wells for all compositions. In addition, since the Al incorporation compared to that of Ga is more sensitive to the NH_3 flow, we have maintained a constant TMAl flow at 21.4 μmol/min in the wells and barriers. So, to adjust the required composition for different samples, we changed the flow of TMGa in the range of 10.7–42.8 μmol/min. This procedure was efficient to control the wells composition. However, when we switch off the TMGa in the barriers, the V/III ratio changed from 875 to a different value from 1300 to 2600 depending on the sample (see Fig. 1(b)). As a result, some variation of AlN barriers thickness was observed. This variation has no impact on the barrier height and, hence, it has no effect on the photoluminescence (PL) transition energy in the QWs.

Structural characterization of the four AlGaN/AlN MQWs structures was carried out using Philips X'Pert diffractometer. Symmetric scans were performed in the triple-axis configuration, while asymmetric was carried out in low-resolution mode (1 mm slit in front of the detector) to enhance the signal intensity. Optical transmission in ♯251 and ♯252 structures was measured at 300 K using a Perkin-Elmer spectrophotometer. The transmission intensity was normalized to an empty-hole signal and experimental data were simulated using SCOUT2 software. Dielectric properties of the composite AlN/sapphire substrate were determined from independent reference measurements. Time-integrated PL spectra were collected at room temperature for samples ♯251 and ♯252, using the 213 nm fifth harmonic of a mode-locked Nd:YAG laser with the pulse duration of 30 ps.

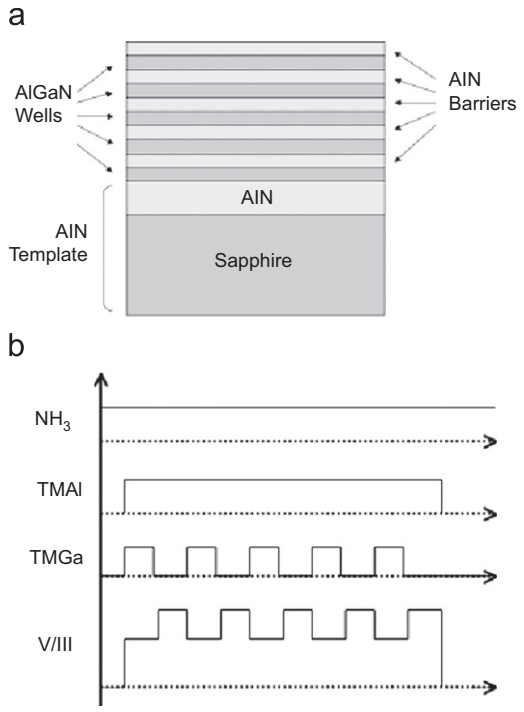

Fig. 1. (a) Schematics of a typical MQW structure and (b) typical feeding sequence during the MQW growth.

3. Results and discussion

Fig. 2 shows $2\theta-\theta$ scans for samples ♯251 and ♯252 measured in the vicinity of the (0 0 .2) reflection of AlN. Diffraction profiles are dominated by the strong peak from AlN pseudo-substrate.

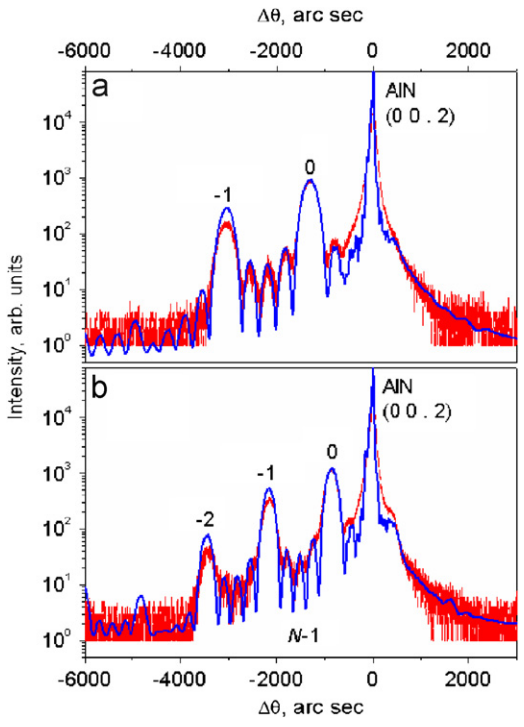

Fig. 2. XRD $2\theta-\theta$ scans for AlGaN/AlN MQWs (a) ♯251 and (b) ♯252 structures. Strong diffraction peak in the center of the spectrum corresponds to the (00.2) reflection of the AlN pseudo bulk substrate, the interstitial N–1 Kiessig fringes (minima), where $N = 5$ is the number of QWs, are also visible. Red curves correspond to experimental data, blue curves are results of simulations.

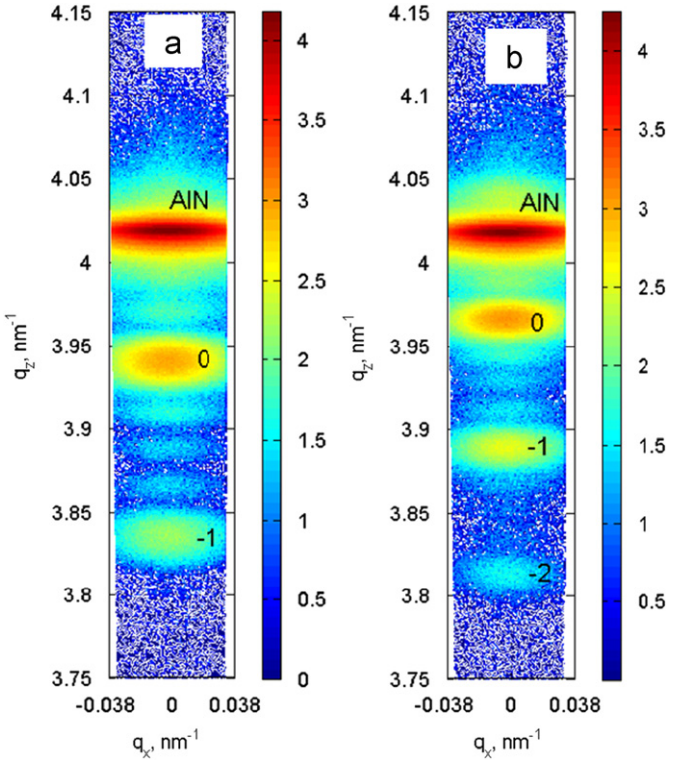

Fig. 3. High-resolution RSM for (0 0 .2) reflection of AlGaN/AlN MQW (a) ♯251 and (b) ♯252 structures. Strong diffraction peak in the center of the map corresponds to the (0 0 .2) reflection of the AlN pseudo bulk substrate. MQW peaks ($\bar{2}$, $\bar{1}$, 0) are marked according to their order.

SL peaks associated with the presence of MQWs structures can be seen for both samples. The interstitial $N-1$ Kiessig fringes (minima), where $N=5$ is the number of QWs, are also visible attesting to the high crystalline quality of the grown structures.

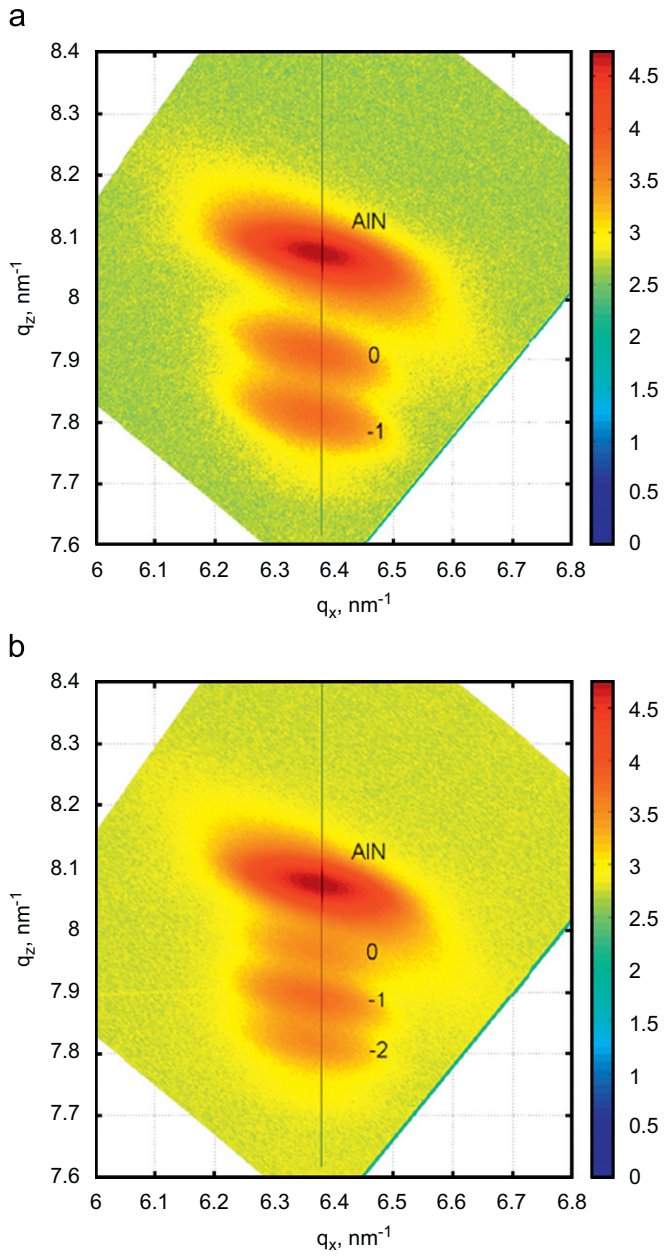

Fig. 4. Low-resolution RSM for (11.4) reflection of AlGaN/AlN MQW (a) ♯251 and (b) ♯252 structures. Strong diffraction peak in the center of the map corresponds to the (11.4) reflection of the AlN pseudo bulk substrate. MQW peaks ($\bar{2}$, $\bar{1}$, 0) are marked according to their order.

MQW periods were determined for our samples by measuring the separation between adjacent SL peaks. The global MQW strain S was determined from the separation between the 0th order SL peak and the AlN substrate peak. In the following, strain is expressed in terms of the d-spacing mismatch in (0 0.1) direction and is calculated with respect to AlN pseudo-substrate layer.

The structural quality of the grown MQW structures has been assessed by reciprocal space mapping (RSM) measured for symmetric (0 0.2) (see Fig. 3) and asymmetric (11.4) reflections (see Fig. 4). The full-width at half-maximum (FWHM) of the rocking curve for the AlGaN layer peak, which is about 0.05°, is close to that of the AlN substrate. The relative orientation of the AlN and MQW peaks in the asymmetric RSMs indicates that the in-plane lattice parameters of the MQWs and the substrate are the same within the accuracy of our low-resolution measurement. Thus, we confirm that the MQWs are elastically strained with respect to AlN substrates.

For simple layers, the composition of the AlGaN can be determined using Vegard's law assuming the layers are fully strained or fully relaxed, but if the strain is partially relaxed, i.e. the degree of relaxation is unknown, the composition cannot be accurately determined. The determination is getting even more inaccurate with a multi-layer structure because of the increases of the number of its parameters. Nevertheless, with the results obtained from RSM, specially knowing that the structure is 100% strained, thicknesses and composition of the wells and barriers were accurately determined using Panalytical Expert Epitaxy software. The resulting parameters of the four MQW structures examined are summarized in Table 1.

The Al composition in the solid phase of QWs is plotted in Fig. 5 as a function of the TMAl/(TMAl+TMGa) ratio. The behaviour is mostly linear. In addition, AlGaN growth rate, depicted in the inset of Fig. 5 is linearly governed by the total III elements flow

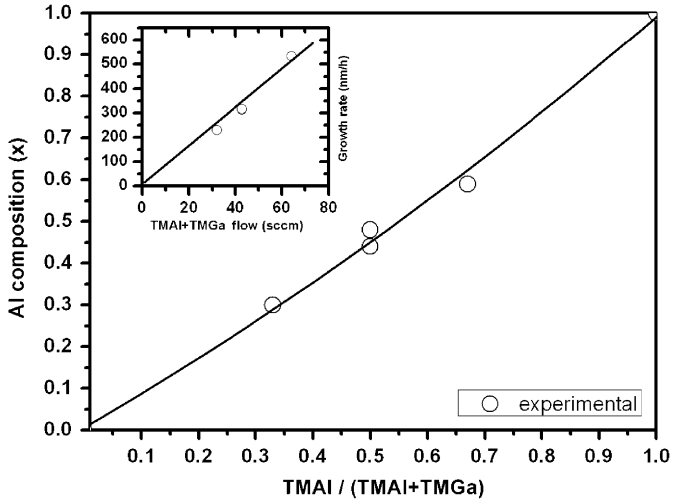

Fig. 5. Al composition plotted in function of TMAl/(TMAl+TMGa) ratio. Solid line is a guide for the eyes. Inset depicts AlGaN growth rate vs. TMAl+TMGa flow.

Table 1
MQWs structures parameters extracted from XRD measurements

Sample ID	Well Al ratio (x)	Well thickness (nm)	Barrier thickness (nm)	AlGaN growth rate (nm/h)	AlN growth rate (nm/h)	Well strain in the (0 0 1) direction (%)
♯251	0.44	6.2	3.3	314	152	3
♯252	0.48	6.2	6.67	314	154	2.7
♯322	0.59	5.1	6.35	230	147	4.02
♯323	0.3	4.0	9.2	533	137	2.05

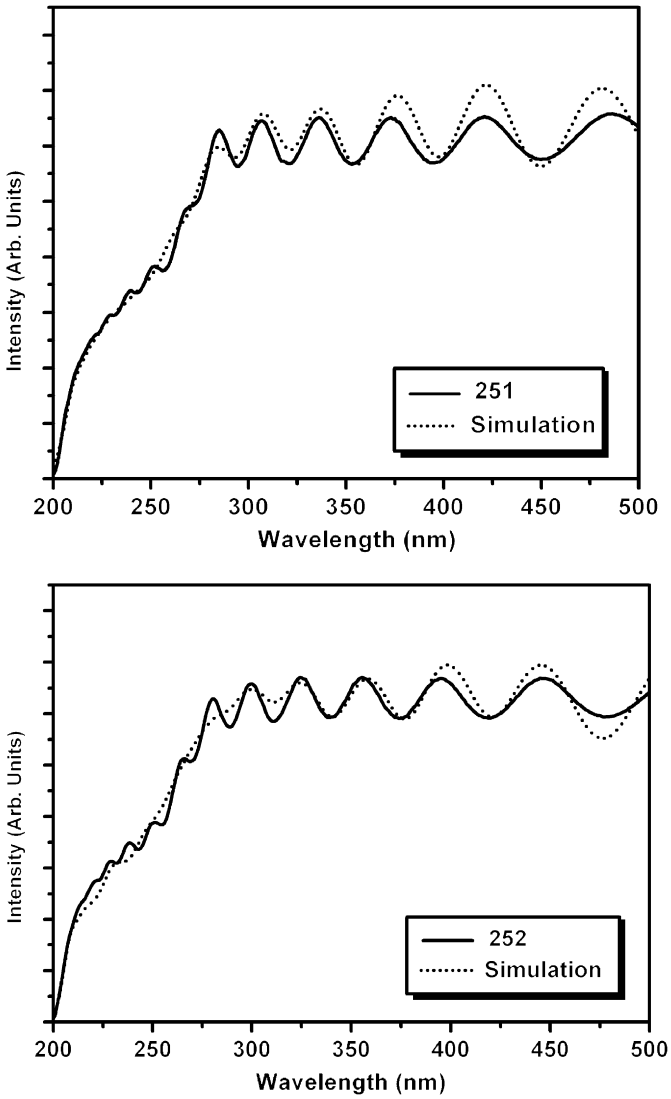

Fig. 6. Transmission spectra of samples ♯251 and ♯252. Solid curves are the experimental data and dotted ones are simulations.

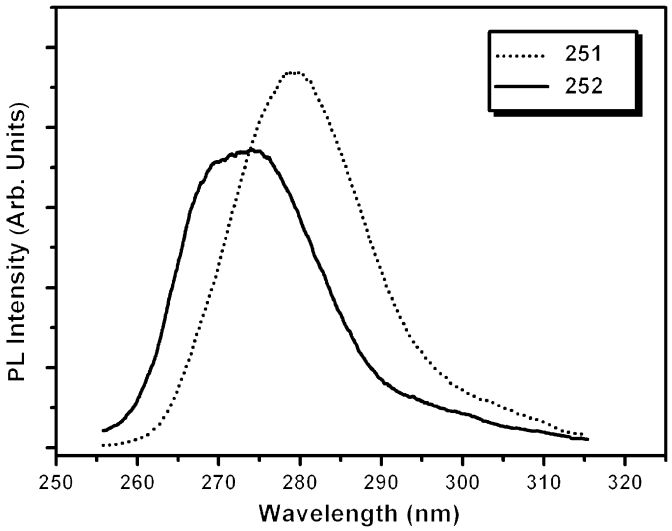

Fig. 7. PL spectra of MQW samples ♯251 and ♯252 with an excitation by the 5th harmonic (213 nm) of a mode-locked Nd:YAG laser (power density was 380 MW/cm^2). Spectra are time integrated.

(TMAl+TMGa), that attests that our conditions were optimized to achieve both composition and thickness control during the growth of QWs. However, although we have used constant TMAl flow for the barriers, the AlN growth rate exhibited a slight decrease probably imputable to the increases of the V/III ratio [11], but, as mentioned above, it has no effect on the height of the barrier.

Optical characterization using white-light transmission and PL was performed on samples ♯251 and ♯252. Results of optical transmission measurements are shown in Fig. 6 for both samples ♯251 and ♯252. In order to extract the optical bandgap values from transmission profiles, experimental data were fitted using the OJL model [12] for interband transitions in disordered materials that included composition and thickness fluctuations responsible for an inhomogeneous broadening for AlGaN layers. This approach allowed us to decouple two contributions to the bandgap absorption threshold originated from the compositional disorder and the shift of the bandgap due to the confinement and composition variation. The first contribution is described by the parameter "gamma", which is close for both structures to 0.19 eV (~13 nm). The optical bandgaps were determined to be at 288 nm for ♯251 and 280 nm for ♯252 that corresponded to the bandgap difference for two structures of about 0.123 eV.

The PL spectra of ♯251 and ♯252 at room temperature are shown in Fig. 7. The maximum of the PL intensity is slightly blue-shifted compared to the transmittance edge. This blue-shift can be explained by the photo-excited carrier screening effect of the strain-induced piezo-electric field. This screening effect is due to the high excitation power, which in our case is 380 MW/cm^2. From these observations, the PL transitions are 280 nm for ♯251 and 273 nm for ♯252. In order to compare our PL measurements to the theoretical values, the QWs transition energies were extracted from envelope function calculations using the transfer-matrix method [13]. In this model, both the piezo-electric field and the exciton binding energy are included. Fig. 8 shows the calculated variation of PL transition vs. piezo-electrical field. For comparison, the measured bandgaps from both PL and transmission of samples ♯251 and ♯252 (horizontal lines) are plotted in the same figure. A good fit between the simulation and measurements is obtained for the field value of 900 and 930 kV/cm, respectively. Marcinkevicius et al. [14] reported similar values of electric field for AlGaN MQW. On the other hand, these numbers are much smaller than the electric field obtained from the theoretical expressions

$$P_{\text{total}} = 2\frac{a-a_0}{a_0}\left(e_{31} - e_{33}\frac{C_{13}}{C_{33}}\right) + P_{\text{sp}}, \quad F = -\frac{P_{\text{total}}}{\varepsilon_r \varepsilon_0},$$

where P_{total} is the total polarization in the well and F the electric field in the (00.1) direction. This discrepancy has been reported by several authors [14,15] and has been attributed to the uncertainty of the theoretical calculations due to strains, spatially localized exciton states, or impurities in investigated materials.

4. Conclusions

AlGaN/GaN MQWs were grown using nitrogen as carrier gas on AlN pseudo bulk substrates. Structural and optical parameters of MQWs have been determined using XRD, transmission and PL spectroscopy. From RSM measurements, we conclude that the MQWs are elastically strained. XRD profiles comprise SL peaks from order 0 to −2 substantiating good interface quality between AlGaN wells and AlN barriers in the MQWs promoted by the use of

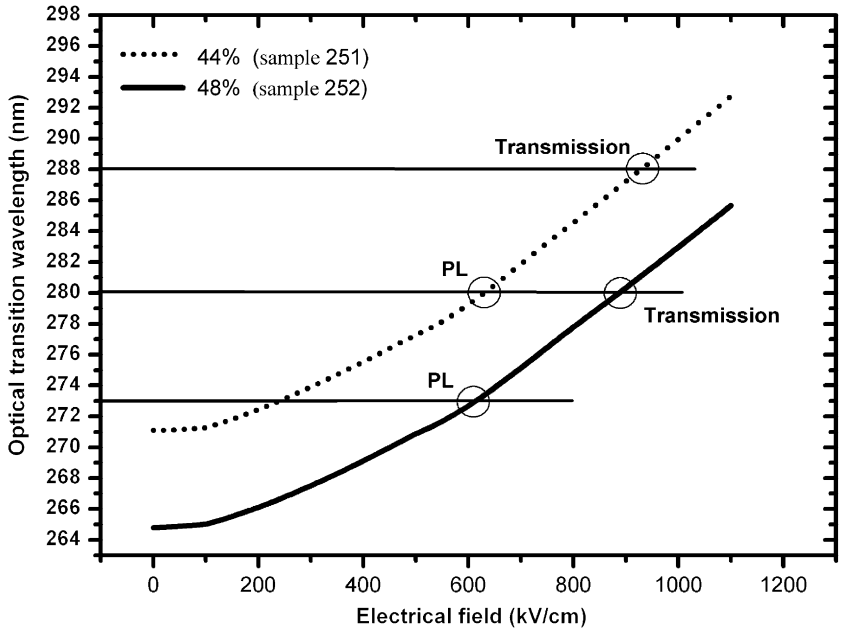

Fig. 8. Room-temperature PL transition wavelength plotted as a function of piezo-electrical field in the MQWs. Dotted line corresponds to sample ♯251 and solid one to sample ♯252. Also, the horizontal lines depict the bandgap energies (wavelengths) determined by both PL and transmittance measurements.

nitrogen as carrier gas. Keeping the V/III ratio and TMAl flow constant during the wells growth allowed to control the Al composition in a wide range. PL and transmission measurements gave an estimation of the internal piezo-electric field of about 900 kV/cm in $Al_{0.44}Ga_{0.56}N$/AlN QW.

Acknowledgements

The authors thank R.D. Dupuis and J.H. Ryou for providing high-quality AlN templates. The authors are thankful to S. Dalmasso from University of Metz for useful discussions. J. Vetyzou is also acknowledged for technical assistance.

References

[1] S.J. Hearne, J. Han, S.R. Lee, J.A. Floro, D.M. Follstaedt, E. Chason, I.S.T. Tsong, Appl. Phys. Lett. 76 (2000) 1534.
[2] T. Sugahara, H. Sato, M. Hao, Y. Naoi, S. Kurai, S. Tottori, K. Yamashita, K. Nishino, L.T. Romano, S. Sakai, Jpn. J. Appl. Phys. 37 (1998) L398.
[3] Da-Bing Li, M. Aoki, T. Katsuno, H. Miyake, K. Hiramatsu, T. Shibata, J. Crystal Growth 298 (2007) 500.
[4] S. Sumiya, Y. Zhu, J. Zhang, K. Kosaka, M. Miyoshi, T. Shibata, M. Tanaka, T. Egawa, Jpn. J. Appl. Phys. 47 (2008) 43.
[5] K. Nagamatsu, N. Okada, H. Sugimura, H. Tsuzuki, F. Mori, K. Iidaa, A. Bando, M. Iwaya, S. Kamiyama, H. Amano, I. Akasaki, J. Crystal Growth 310 (2008) 2326.
[6] R. Gaska, C. Chen, J. Yang, E. Kuokstis, A. Khan, G. Tamulaitis, I. Yilmaz, M.S. Shur, J.C. Rojo, L.J. Schowalter, Appl. Phys. Lett. 81 (2002) 4658.
[7] J.R. Creighton, W.G. Breiland, M.E. Coltrin, R.P. Pawlowski, Appl. Phys. Lett. 81 (2002) 2626.
[8] A.V. Kondratyev, R.A. Talalaev, W.V. Lundin, A.V. Sakharov, A.V. Tsatsul'nikov, E.E. Zavarin, A.V. Fomin, D.S. Sizov, J. Crystal Growth 272 (2004) 420.
[9] S. Yamaguchi, M. Kariya, S. Nitta, T. Kashima, M. Kosaki, Y. Yukawa, H. Amano, I. Akasaki, J. Crystal Growth 221 (2000) 327.
[10] S. Gautier, C. Sartel, S. Ould-Saad, J. Martin, A. Sirenko, A. Ougazzaden, J. Crystal Growth 298 (2007) 428.
[11] A.V. Lobanova, K.M. Mazaev, R.A. Talalaev, M. Leys, S. Boeykens, J. Crystal Growth 287 (2006) 601.
[12] S.K. O'Leary, S.R. Johnson, P.K. Lim, J. Appl. Phys. 82 (1997) 3334.
[13] N. Grandjean, B. Damilano, S. Dalmasso, M. Leroux, M. Laugt, J. Massies, J. Appl. Phys. 86 (1999) 3714.
[14] S. Marcinkevicius, A. Pinos, K. Liu, D. Veksler, M.S. Shur, J. Zhang, R. Gaska, Appl. Phys. Lett. vol. 90 (2007) 081914.
[15] H. Teisseyre, T. Suski, S.P. epkowski, S. Anceau, P. Perlin, P. Lefebvre, L. Koczewicz, H. Hirayama, Y. Aoyagi, et al., Appl. Phys. Lett. 82 (2003) 1541.